

---

# A DIGITALIZED ATLAS FOR PULMONARY AIRWAY

---

A PREPRINT

Minghui Zhang, Chenyu Li, Hanxiao Zhang, Yaoyu Liu, Yun Gu  
Institute of Medical Robotics  
Shanghai Jiao Tong University  
Shanghai, China

## ABSTRACT

Pulmonary airway is an important anatomy. In this work, we proposed *AirwayAtlas*, which is an end-to-end pipeline for automatic extraction of airway anatomies with lobar, segmental and subsegmental labeling. A compact representation, *AirwaySign*, is generated based on diverse features of airway branches. Experiments on multi-center datasets validated the effectiveness of *AirwayAtlas*. We also demonstrated that *AirwaySign* is a powerful tool for correlation analysis on pulmonary diseases. The implementation of key components can be found in <https://github.com/EndoluminalSurgicalVision-IMR>.

## 1 Introduction

The pulmonary airway refers to the network of structures within the respiratory system that conducts air from the external environment to the lungs and facilitates gas exchange. The morphological anatomy of the pulmonary airway includes the detailed structural features of the airway, which are critical for diagnosing respiratory diseases. It is also the natural path for endobronchial biopsy and treatment. Due to the complex structure of airway, it is however challenging to manually annotate the airway based on medical imagings, which cannot fully extract the fine-grained distal bronchi and time-consuming. Without large-scaled and detailed annotation of airways, it is also difficult to analyze the distribution of anatomical variations and correlation of diseases. Therefore, previous works only focus on the statics of certain regions, like left upper lobe [He et al., 2022, Deng et al., 2022], right lower lobe [Zhu et al., 2023], with manual check of binary airway segmentations.

Recently, the automated methods have been proposed for binary segmentation, lobar/segmental and subsegmental labeling of airway. Previous airway segmentation benchmarks [Lo et al., 2012, Zhang et al., 2023, Nan et al., 2024] and methods [Charbonnier et al., 2017, Xu et al., 2015, Meng et al., 2017, Qin et al., 2019, Nadeem et al., 2020a, Zheng et al., 2021, Nan et al., 2023, Zhang and Gu, 2023, Wang et al., 2024] lack a fine-grained evaluation of airway reconstruction. In many cases, assessing the overall quality of airway reconstruction may not be necessary. Instead, the reconstruction quality of local segments and subsegments surrounding lesions is of greater clinical importance. Therefore, branch-wise detailed evaluation holds significant relevance for clinical applications.

Recent approaches to airway anatomical labeling face several limitations that prevent them from automatically achieving subsegmental-level labeling. Most works rely on the ground truth airway shape to predict segmental-level anatomical labeling [Xie et al., 2025, Huang et al., 2024]. While Yu et al. [2022a] extends to subsegmental classification, it depends heavily on ground truth data annotated from CT images and manually refined features, rendering it incapable of operating directly from raw CT scans. This reliance diminishes its clinical applicability. Only a few works [Nadeem et al., 2020b, Xie et al., 2024, Chau et al., 2024] attempt to directly infer anatomical airway labeling from CT scans. However, these methods are limited to incomplete segmental-level anatomical labeling on relatively small-scale datasets, further highlighting the gap in achieving comprehensive, automated airway labeling.

In this work, we proposed *AirwayAtlas*, a digitalized atlas for pulmonary airway, and *AirwaySign*, a compact representation based on diverse features of airway. The contributions of the this work are three-folded:

- **Data:** We constructed the largest multi-center dataset to build the digitalized atlas of pulmonary airway. It is labeled with subsegmental-level bronchi, covering various diseases.

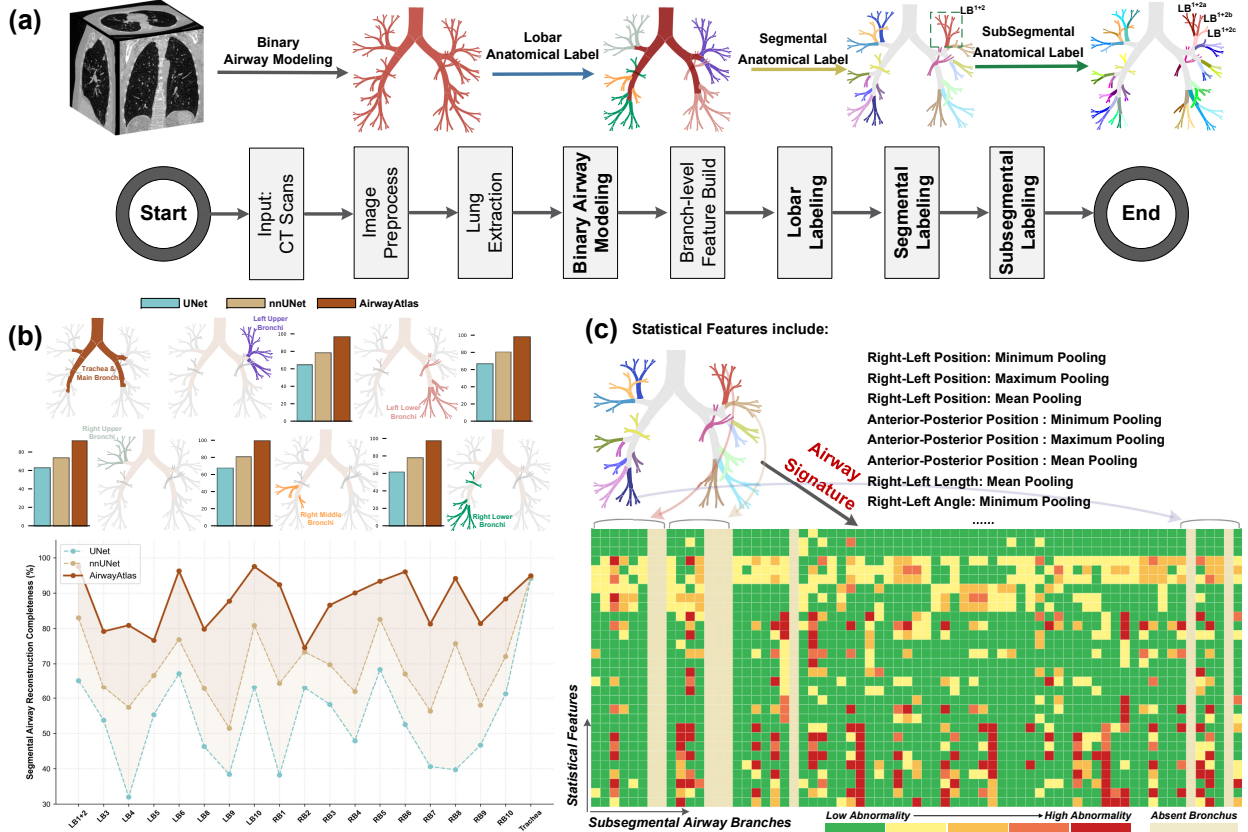


Figure 1: (a) The overall pipeline of the AirwayAtlas. It automatically models binary airway trees from CT scans and extracts branch-level features, enabling the automated identification and labeling of airway anatomies at the lobar, segmental, and subsegmental levels; (b) Evaluation from binary segmentation to anatomical labeling among the baseline methods and AirwayAtlas. It can be observed that AirwayAtlas can significantly improve the recognition of the small distal airway; (c) AirwaySign serves as a compact representation of the volumetric image and anatomical airway. It integrates structural and morphological features at the subsegmental level, enabling clinicians to perform correlation analyses between pulmonary diseases and specific regions of interest within images and airways.

- **Method:** An end-to-end airway labeling model is proposed, allowing direct inference from the CT image to the detailed airway labels.
- **Results:** The model is evaluated with the large-scale dataset, including: 1) Fine-grained labeling of the airway atlas; 2) Statistics on bronchi branching pattern; and, 3) Correlation between pulmonary diseases and AirwaySign.

## 2 Method

In this study, we first introduce AirwayAtlas, an end-to-end framework for anatomical labeling of airways, which could be seen in Fig.1. AirwayAtlas automatically models binary airway trees from CT scans and extracts branch-level features, enabling the automated identification and labeling of airway anatomies at the lobar, segmental, and subsegmental levels. AirwayAtlas provides the most detailed anatomical labeling, including 6 types of lobar bronchi, 19 types of segmental bronchi, and 127 types of subsegmental bronchi. We further propose AirwaySign, a compact and informative representation of airway anatomy. Based on the results from airway anatomical labeling, AirwaySign integrates structural and morphological features at the subsegmental level. This representation enables clinicians to perform correlation analyses between pulmonary diseases and specific regions of interest within CT scans and anatomical airways, without the need to review the full image set manually or search exhaustively for airway-related abnormalities.

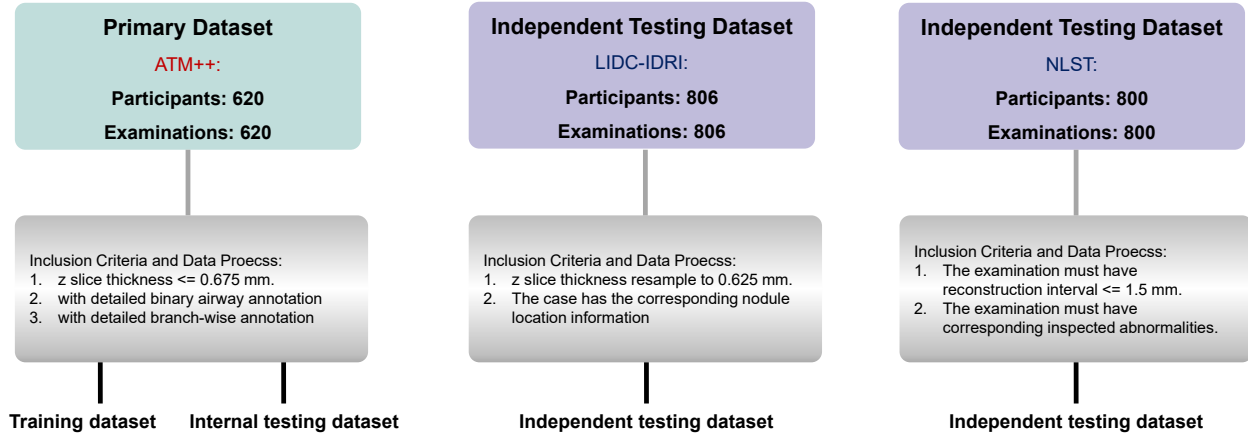


Figure 2: The datasets used for the digitized atlas of the pulmonary airway include ATM++, LIDC-IDRI, and NLST. The ATM++ serves as the primary dataset, which provides 620 patients with detailed annotations for both binary airway labels and subsegmental-level anatomical labels. Approximately 800 patients with lung nodules from the LIDC-IDRI dataset are included in this study. Another 800 patients from the NLST dataset, presenting with conditions such as emphysema and reticular/reticulonodular opacities, are also selected.

## 2.1 AirwayAtlas: A Fine-grained Automated Labeling Pipeline

Building on the success of ATM’22 [Zhang et al., 2023], we adopt the consensus of effective strategies for binary airway tree modeling as the intermediary output of AirwayAtlas. Specifically, we utilize 3D U-Net [Çiçek et al., 2016] and WingsNet [Zheng et al., 2021] as backbone architectures, incorporating novel objective functions such as Connectivity-Aware Loss (CAL) [Zhang and Gu, 2023], General Union Loss (GUL) [Zheng et al., 2021], and Breakage-Sensitive Loss (BS) [Yu et al., 2022b]. These loss functions prioritize topological completeness and correctness, effectively addressing challenges such as leakage and breakage in binary airway tree modeling. An ensemble approach is employed to integrate different models, enhancing robustness in binary airway tree modeling. Additionally, supplementary information, such as training set labels, is utilized to improve intra-class discrimination. Specifically, we apply over-sampling techniques to emphasize peripheral airways, guided by the centerline points ratio. A multi-stage solution is also incorporated into our framework: lung region extraction is used as a hard attention mechanism to focus on relevant areas, mitigating leakage challenges. Furthermore, preliminary predictions from early training epochs provide valuable insights for subsequent epochs, enabling well-directed sampling of difficult patches.

After obtaining the intermediary binary airway, the minimum-cost path-based tree structure extraction method [Sato et al., 2000] is employed to determine the robust skeleton of the airway. Subsequently, inspired by previous studies [Mori et al., 2009, Lo et al., 2011, Yu et al., 2022a], seventeen branch-level quantitative features are extracted from the binary airway and its corresponding skeleton. These features are transformed into a graph-based representation, which serves as input for the subsequent airway anatomical labeling.

To the best of our knowledge, AirwayAtlas represents the first attempt to generate airway anatomical structures through a fully automated, end-to-end framework, initiating with lobar labeling and progressing to a detailed subsegmental delineation. In contrast to previous studies [Nadeem et al., 2020b], which only anatomically labeled a small portion of the predicted airway, and other works [Huang et al., 2024, Xie et al., 2024, 2025] that bypass the original CT images and instead perform segmental-level anatomical labeling using airway volumes or point clouds, AirwayAtlas operates directly from the CT scans, ensuring a more complete and detailed representation of airway anatomy. To handle the diversity of airways extracted from patients with varying levels of disease severity, AirwayAtlas is designed to enhance the consistency of anatomical labeling. Based on our recent work [Li et al., 2024], we integrate hierarchical relationships into a U-shaped transformer block-based framework, enabling a progressive improvement in classification accuracy. Further, to mitigate the substantial inter-individual variability, a soft-subtree consistency module is introduced to encapsulate clinically meaningful anatomical information by organizing segmental branches into subtrees, thereby enhancing the structural consistency across varying cases. Additionally, to address cases involving abnormal bronchial structures, we propose an abnormal branch saliency method to identify branches that cannot be classified into any category within the established nomenclature [Netter, 2014]. A detailed implementation of AirwayAtlas can be found

Table 1: Fine-grained evaluation of the binary airway modeling and the anatomical airway labeling. The evaluation covers from the lobar level to the subsegmental level. Tree length detected rate (TD, %) is chosen for the evaluation of the binary airway modeling and the Accuracy (Acc, %) is adopted for the evaluation of the anatomical airway labeling.

Binary Airway Model				Anatomical Airway Labeling			
Method	Lobar	Segmental	Subsegmental	Method	Lobar	Segmental	Subsegmental
UNet	68.81	54.31	43.91	GCN	98.00	85.40	60.20
nnUNet	80.40	69.41	55.33	TNN	97.86	88.80	77.35
AirwayAtlas	<b>95.65</b>	<b>87.83</b>	<b>67.87</b>	AirwayAtlas	<b>99.00</b>	<b>96.89</b>	<b>93.16</b>

in [Zhang and Gu, 2023, Yu et al., 2022b, Zheng et al., 2021, Li et al., 2024], and is also planned to be available at this repository<sup>1</sup>.

## 2.2 AirwaySign: A Compact Representation of Airway Characteristics

By obtaining anatomical airway labeling results aligned with CT images, the analysis of airway morphological changes, coupled with variations in image attributes, can assist clinicians in diagnosing related diseases. However, AirwayAtlas delineates up to 127 distinct subsegmental types of bronchi, providing a vast amount of information. While this wealth of information is valuable, it may increase the diagnostic burden for clinicians. This is primarily due to the fact that examining the volumetric data is memory-intensive and not intuitive. Clinicians often need to rotate the rendered airway structures to identify abnormal branches while simultaneously examining the corresponding characteristics in the image slices by scrolling through stacks of sectional images. Furthermore, it is challenging to observe similar diseased regions concurrently, which adds complexity to the correlation analysis within the same patient.

Inspired by Eisen et al. [1998], we propose AirwaySign to mitigate the aforementioned challenges. As illustrated in Fig.1(c), AirwaySign is constructed based on the output of AirwayAtlas by quantifying the multidimensional characteristics of all 127 subsegmental bronchial types into a single, comprehensive signature matrix. In this matrix, the horizontal axis represents individual subsegmental bronchi, while the vertical axis denotes their statistical features. Currently, we identify thirty structural and morphological characteristics, including right-left position, anterior-posterior position, superior-inferior position, branch length, right-left projection length, anterior-posterior projection length, superior-inferior projection length, , as well as right-left, anterior-posterior, and superior-inferior projection angles. Each characteristic is computed using three aggregation methods: minimum, mean, and maximum pooling, applied within each subsegmental bronchus. Each colored cell within the matrix corresponds to a specific dimensional feature of a particular subsegmental bronchus. The color gradient from green to red indicates an increasing risk of abnormality, while absent branches are represented by a distinct color. The AirwaySign consolidates volumetric imaging and anatomical information into a compact representation, highlighting coherent patterns within the patient. This approach allows clinicians to intuitively identify abnormal branches and focus on specific regions of interest, eliminating the need to search from the entire image. Additionally, AirwaySign facilitates the clustering of different bronchi regions associated with the same disease for more streamlined analysis.

## 3 Material

In this study, we adopted over **2,000** chest CT images representing various diseases to construct the largest digitized atlas of the pulmonary airway. The images were categorized into a primary dataset and two independent testing datasets. The primary dataset was utilized to optimize AirwayAtlas and AirwaySign, while the two independent testing datasets were designated for clinical correlation analyses of pulmonary diseases associated with the anatomical airways and their surrounding structures.

**ATM++ Dataset:** ATM++ integrated the ATM’22 [Zhang et al., 2023] and AIIB’23 [Nan et al., 2024] dataset, both of which have the binary airway annotation. ATM’22 includes 500 CT scans with annotation in total and AIIB’23 provides 120 training cases with annotation. We extends these 620 CT scans from binary airway annotation to the detailed anatomical delineation, including 6 types of lobar bronchi, 19 types of segmental bronchi, and 127 types of subsegmental bronchi. These anatomical labels were carefully delineated and manually verified by three radiologists with over five years of professional experience. Regarding the initial resolution of ATM++, each chest CT scan from ATM’22 contains a variable number of slices, ranging from 157 to 1125, with a slice thickness of 0.450 to 1.000 mm. The axial resolution of all slices is  $512 \times 512$  pixels, with a spatial resolution between 0.500 and 0.919 mm. Similarly,

<sup>1</sup><https://github.com/EndoluminalSurgicalVision-IMR/ATM-22-Related-Work>



Figure 3: Visualization of the detailed evaluation of the AirwayAtlas on representative subsegmental bronchi. The tree length detection rate (TD, %) is used as the measurement metric. AirwayAtlas is compared with UNet and nnUNet.

AIIB'23 includes cases where the number of slices exceeds 120, each measuring over  $512 \times 512$  pixels, with a spatial resolution of 0.417 to 0.926 mm. The number of slices in AIIB'23 ranges from 146 to 947, with a slice thickness of 0.400 to 2.000 mm.

**LIDC-IDRI Dataset:** The Lung Image Database Consortium and Image Database Resource Initiative (LIDC-IDRI) [Armato III et al., 2011, 2015] is a widely recognized public chest CT dataset used for lung nodule detection, classification, and quantitative assessment. The LIDC-IDRI database comprises 1,018 cases, each containing a clinical thoracic CT scan along with an associated XML file that documents nodule-related information. The slice thickness in the LIDC-IDRI dataset varies from 0.6 to 3.0 mm. ATM'22 has already included 140 CT scans from the LIDC-IDRI dataset, and we selected approximately 800 additional CT scans for our study based on image quality. The slice thickness of these selected CT scans was uniformly resampled to 0.625 mm.

**NLST Dataset:** The National Lung Screening Trial (NLST) [Team, 2011, 2013] is one of the largest lung cancer

screening trials, conducted between 2002 and 2004. NLST enrolled 53,454 individuals at high risk for lung cancer across 33 U.S. medical centers. For this study, we selected approximately 800 CT scans based on the following criteria: 1) The CT scan includes corresponding documented abnormalities. A diverse range of diseases was carefully considered, including non-calcified nodules or masses, non-calcified micronodules, atelectasis, consolidation, emphysema, and reticular/reticulonodular opacities. 2) The CT scan must have a reconstruction interval of less than 1.5 mm, with no empty or zero interval values. The slice thickness of these selected CT scans is then uniformly resampled to 0.625 mm. 3) Only one examination per patient per study year is included. The selection is based on the following criteria: the minimum reconstruction interval, the most optimal reconstruction filter, and the maximum number of slices.

## 4 Experiments

### 4.1 Validation: Fine-grained Evaluation of AirwayAtlas

Unlike previous airway segmentation benchmarks [Lo et al., 2012, Zhang et al., 2023, Nan et al., 2024], they only reported the global binary tree length detection rate and branch detection rate for the entire airway tree. This statistical approach does not evaluate the detection completeness of specific bronchial segments or subsegments with clinical anatomical relevance. This is particularly crucial in disease-oriented contexts, where path planning to the lesion area is required. Under this situation, the focus is on the completeness of detection in regions such as the bronchi surrounding nodules. Hence, we conducted a fine-grained evaluation of AirwayAtlas, which includes both the performance of the binary airway model and the anatomical airway labeling, as presented in Table 1.

The *tree length detection rate* [Zhang et al., 2023] (TD, %) is used to evaluate the completeness of the binary airway tree at the lobar, segmental, and subsegmental bronchi levels. The *accuracy* [Li et al., 2024] is employed to assess the correctness of the anatomical labeling at these same levels. Based on the results presented in Table 1, AirwayAtlas demonstrates a significant performance advantage over both UNet [Çiçek et al., 2016] and nnUNet [Isensee et al., 2021] in the evaluation of binary airway segmentation and anatomical airway labeling. In terms of TD, AirwayAtlas achieves a superior detection rate across all airway levels. For the lobar level, AirwayAtlas reaches 95.65%, significantly outperforming UNet (68.81%) and nnUNet (80.40%). At the segmental level, AirwayAtlas achieves 87.83%, while UNet and nnUNet report 54.31% and 69.41%, respectively. For the subsegmental level, AirwayAtlas shows a detection rate of 67.87%, compared to 43.91% for UNet and 55.33% for nnUNet. These results highlight AirwayAtlas’s enhanced ability to capture finer details of the airway structure, revealing its significant potential in reaching distal lesions and demonstrating its high clinical value. Furthermore, AirwayAtlas outperforms both GCN [Kipf and Welling, 2017] and TNN [Yu et al., 2022a] in terms of accuracy for anatomical airway labeling. AirwayAtlas achieves over 90% accuracy across all lobar, segmental, and subsegmental bronchial levels, with accuracy exceeding 95% at both the lobar and segmental levels. In contrast, GCN and TNN achieve less than 90% accuracy at the lobar level and less than 80% at the segmental level. This advantage underscores AirwayAtlas’s superior precision in identifying detailed bronchial structures, which, especially when lesions are located near the small airways, increases the accessibility for preoperative planning in endoscopic navigation surgery.

Fig. 3 visualizes the detailed evaluation of AirwayAtlas on representative subsegmental bronchi. The improvement in AirwayAtlas performance is consistent across all subsegmental bronchi. This detailed evaluation is clinically significant, as it allows clinicians to focus on branches related to the disease without the need to examine all branches.

### 4.2 Application: Statistics on bronchi branching pattern

Based on the AirwayAtlas, conducting statistical analysis of the bronchial branching patterns across all five lobes, down to the subsegmental bronchi level, is both time-efficient and feasible. As shown in Fig. 4, we present the statistical data on the lobar-to-segmental and segmental-to-subsegmental branching patterns derived from the primary dataset. The observed branching patterns align closely with those reported in previous studies [Deng et al., 2022, He et al., 2022], which only focused on the bronchial branching patterns within individual lobes. One key advantage of using AirwayAtlas is its ability to efficiently incorporate new cases, eliminating the need for manual verification of the binary airway tree to obtain the branching patterns. This automated feature enhances both the efficiency and scalability of conducting large-scale anatomical studies of the bronchial tree.

### 4.3 Application: Correlation between pulmonary diseases and AirwaySign

Fig. 5 illustrates the AirwaySign is a compact and powerful tool for correlation analysis on pulmonary diseases. It comprises three distinct case studies, each demonstrating how AirwaySign patterns relate to underlying lung conditions as confirmed by three-dimensional anatomical reconstructions and corresponding CT scan patches. The first row displays a patient with mild abnormalities, and the highlighted subsection within the AirwaySign corresponds to specific



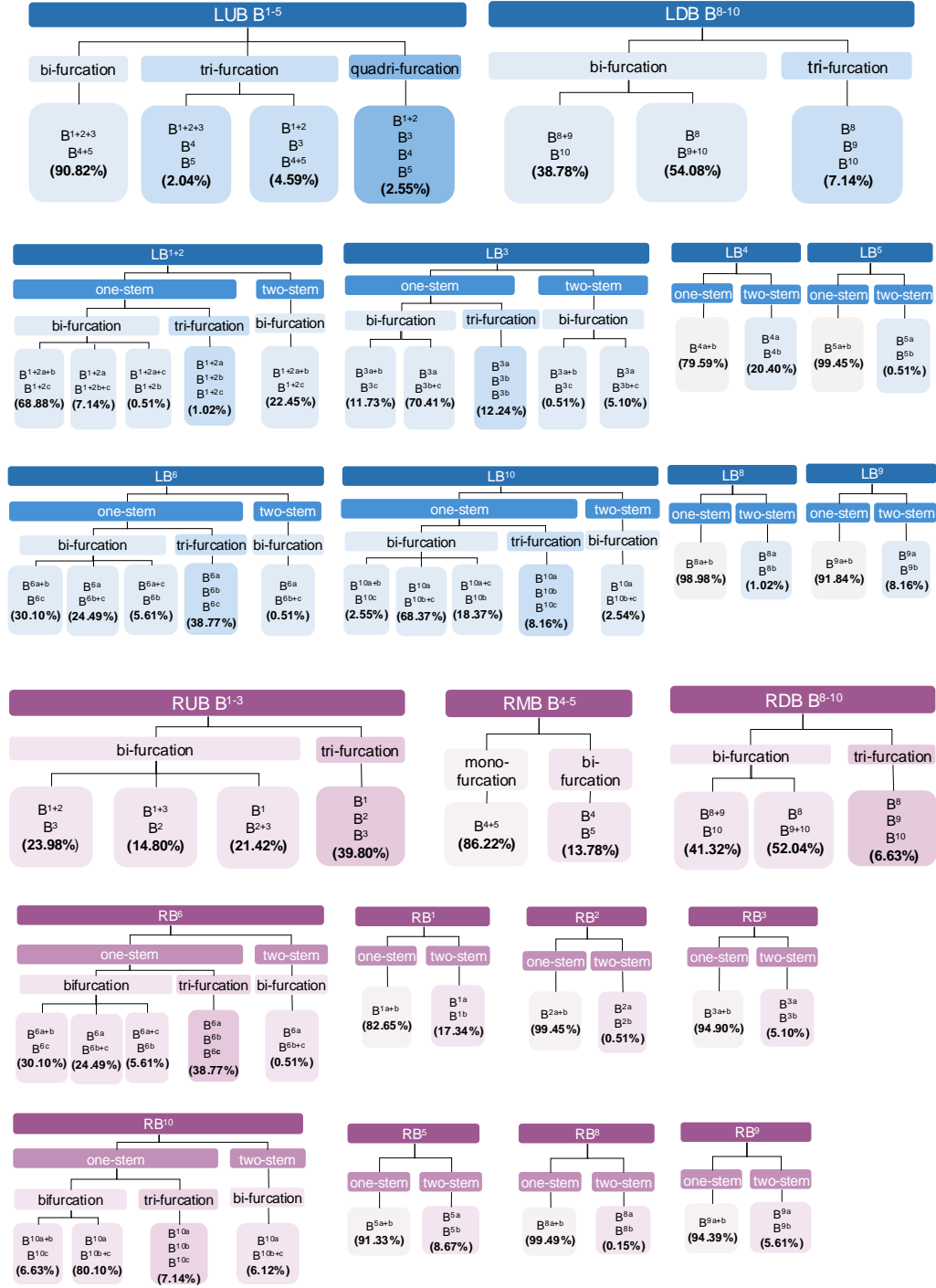


Figure 4: Statistics on bronchi branching pattern across all five lobes, down to the subsegmental bronchi level.

lobar airways (LB8, LB9, LB10) identified in the anatomical airway patch. This segment of the airway tree, upon inspection of the CT images, exhibits a structurally preserved pattern consistent with normal pulmonary anatomy. The CT scan patch reinforces this assessment. Hence, in Case 1, the relatively uniform and predominantly green distribution of AirwaySign values signifies minimal pulmonary related disease risk.

Contrastingly, the AirwaySign of Case 2 demonstrates a more heterogeneous and predominantly red pattern in the highlighted airway segments (LB8, LB9, LB10), indicative of pronounced morphological deviations from the normal

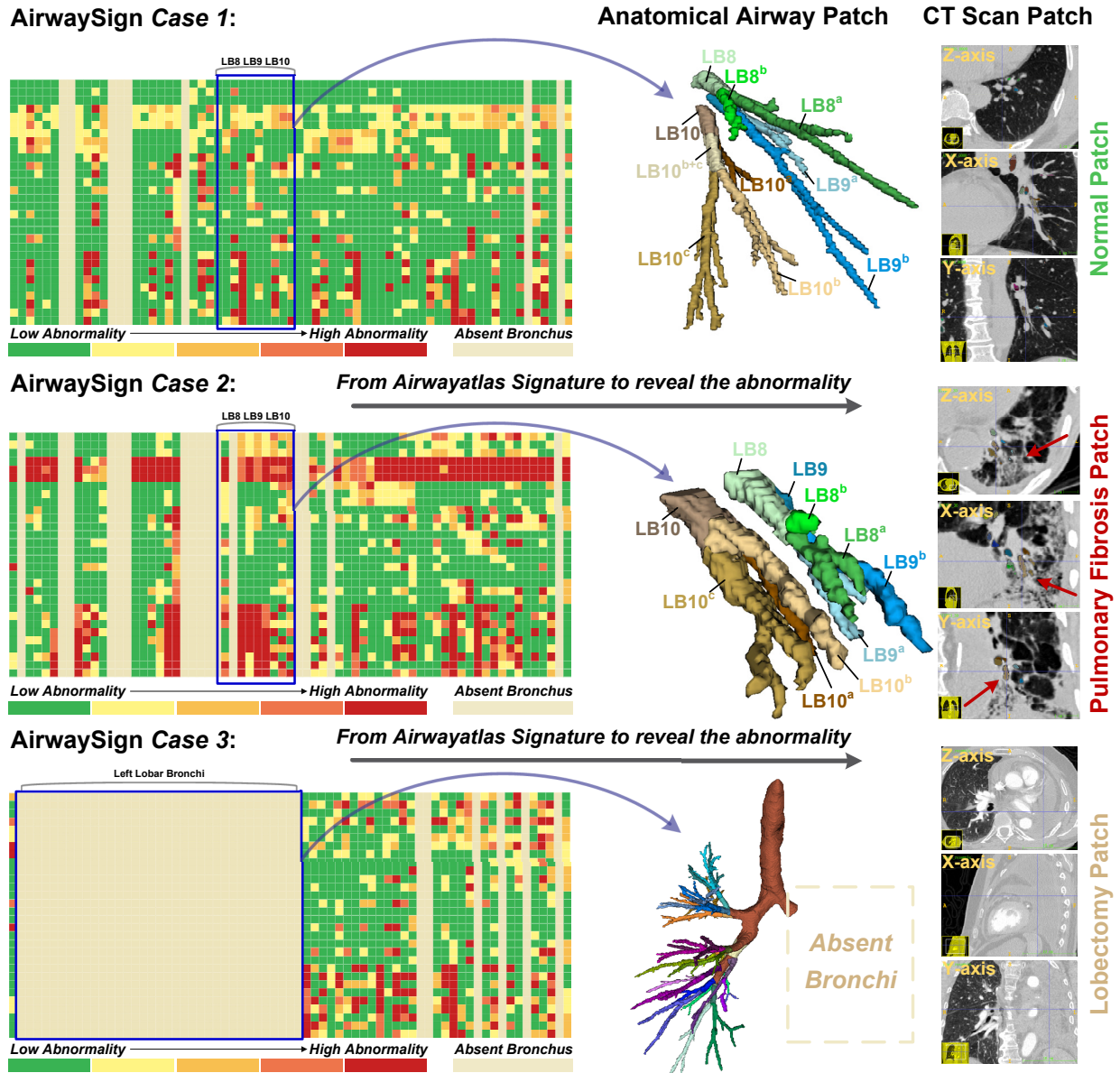


Figure 5: Correlation analysis between pulmonary diseases and AirwaySign. The first row displays a patient with mild abnormalities. The second row presents a patient with pulmonary fibrosis. The third row depicts a patient who has undergone a left lobectomy. This figure is best viewed in color.

AirwayAtlas. The corresponding volumetric anatomical reconstruction shows the deformation of the segmental bronchi. Correlative CT scan patches reveal typical features of fibrotic lung disease. The elevated abnormality signals captured in the AirwaySign align with these radiological findings, confirming that variations in airway geometry—such as abnormal branching angles or segmental volume loss are closely associated with fibrotic alterations. This illustrates that the characteristics of lung fibrosis could be observed in the AirwaySign.

The third example, AirwaySign captures a scenario with a dramatically altered airway architecture in which an entire left lobe’s bronchial structure is absent due to surgical resection (lobectomy). The absence of airway segments in the highlighted region results in a consistent, featureless field in the AirwaySign. This anatomical disruption is reflected in the three-dimensional model, which shows a truncated airway tree, and is corroborated on CT imaging. The difference between normal and surgically removed segments highlights the utility of AirwaySign as a quantitative tool to identify and localize severe anatomical alterations.



Across these studies, the correlation between the AirwaySign and pulmonary diseases is evident. AirwaySign, derived from AirwayAtlas and mapped onto patient-specific data, not only identifies subtle structural deviations but also localizes them with high specificity. In normal conditions, AirwaySign presents minimal or no deviation, serving as a baseline. In fibrotic disease states, regional increases in airway abnormality scores reflect the structural changes. In cases of anatomical absence, AirwaySign clearly demarcates removed or non-existent airways. These correlations suggest that AirwaySign could be integrated into clinical decision-making, providing a quantitative, visual framework for evaluating the severity and extent of airway pathology.

## 5 Conclusion

In this study, we propose the AirwayAtlas, which represents a significant advancement in the automated analysis of pulmonary airway anatomy. Its ability to deliver fine-grained airway segmentations, supported by the novel AirwaySign representation, enables deeper insights into pulmonary diseases and holds promise for improving clinical diagnostics and research. Furthermore, our study on large-scale datasets, including over 2000 CT scans, demonstrated that AirwayAtlas can effectively handle diverse and complex data, providing robust performance across a variety of diseases. This work sets the foundation for future studies that require detailed and accurate airway modeling, contributing to both pulmonary airway analysis and personalized medicine.

## References

- Hao He, Feng Wang, Pei Yuan Wang, Peng Chen, Wilson WL Li, Gianluca Perroni, and Shuo Yan Liu. Anatomical analysis of variations in the bronchus pattern of the left upper lobe using three-dimensional computed tomography angiography and bronchography. *Annals of Translational Medicine*, 10(6), 2022.
- Youjun Deng, Songhua Cai, Chujian Huang, Wenyi Liu, Longde Du, Chunguang Wang, Ran Jia, Shengcheng Lin, Xin Yu, Xiangyang Yu, et al. Anatomical variation analysis of left upper pulmonary blood vessels and bronchi based on three-dimensional reconstruction of chest ct. *Frontiers in Oncology*, 12:1028467, 2022.
- Shusheng Zhu, Wenzheng Xu, Zhihua Li, Weibing Wu, Alessandro Brunelli, Yosuke Matsuura, Giulio Maurizi, Davide Tosi, Ilies Bouabdallah, Dominique Gossot, et al. Branching patterns and variations of the bronchus and blood vessels in the superior segment of the right lower lobe: a three-dimensional computed tomographic bronchography and angiography study. *Journal of Thoracic Disease*, 15(12):6879, 2023.
- Pechin Lo, Bram Van Ginneken, Joseph M Reinhardt, Tarunashree Yavarna, Pim A De Jong, Benjamin Irving, Catalin Fetita, Margarete Ortner, Rômulo Pinho, Jan Sijbers, et al. Extraction of airways from ct (exact'09). *IEEE Transactions on Medical Imaging*, 31(11):2093–2107, 2012.
- Minghui Zhang, Yangqian Wu, Hanxiao Zhang, Yulei Qin, Hao Zheng, Wen Tang, Corey Arnold, Chenhao Pei, Pengxin Yu, Yang Nan, et al. Multi-site, multi-domain airway tree modeling. *Medical image analysis*, 90:102957, 2023.
- Yang Nan, Xiaodan Xing, Shiyi Wang, Zeyu Tang, Federico N Felder, Sheng Zhang, Roberta Eufrasia Ledda, Xiaoliu Ding, Ruiqi Yu, Weiping Liu, et al. Hunting imaging biomarkers in pulmonary fibrosis: Benchmarks of the aiiib23 challenge. *Medical Image Analysis*, 97:103253, 2024.
- Jean-Paul Charbonnier, Eva M Van Rikxoort, Arnaud AA Setio, Cornelia M Schaefer-Prokop, Bram van Ginneken, and Francesco Ciompi. Improving airway segmentation in computed tomography using leak detection with convolutional networks. *Medical image analysis*, 36:52–60, 2017.
- Ziyue Xu, Ulas Bagci, Brent Foster, Awais Mansoor, Jayaram K Udupa, and Daniel J Mollura. A hybrid method for airway segmentation and automated measurement of bronchial wall thickness on ct. *Medical image analysis*, 24(1): 1–17, 2015.
- Qier Meng, Holger R Roth, Takayuki Kitasaka, Masahiro Oda, Junji Ueno, and Kensaku Mori. Tracking and segmentation of the airways in chest ct using a fully convolutional network. In *Medical Image Computing and Computer-Assisted Intervention- MICCAI 2017: 20th International Conference, Quebec City, QC, Canada, September 11-13, 2017, Proceedings, Part II 20*, pages 198–207. Springer, 2017.
- Yulei Qin, Mingjian Chen, Hao Zheng, Yun Gu, Mali Shen, Jie Yang, Xiaolin Huang, Yue-Min Zhu, and Guang-Zhong Yang. AirwayNet: a voxel-connectivity aware approach for accurate airway segmentation using convolutional neural networks. In *International conference on medical image computing and computer-assisted intervention*, pages 212–220. Springer, 2019.
- Syed Ahmed Nadeem, Eric A Hoffman, Jessica C Sieren, Alejandro P Comellas, Surya P Bhatt, Igor Z Barjaktarevic, Fereidoun Abtin, and Punam K Saha. A ct-based automated algorithm for airway segmentation using freeze-and-grow propagation and deep learning. *IEEE transactions on medical imaging*, 40(1):405–418, 2020a.

- Hao Zheng, Yulei Qin, Yun Gu, Fangfang Xie, Jie Yang, Jiayuan Sun, and Guang-Zhong Yang. Alleviating class-wise gradient imbalance for pulmonary airway segmentation. *IEEE transactions on medical imaging*, 40(9):2452–2462, 2021.
- Yang Nan, Javier Del Ser, Zeyu Tang, Peng Tang, Xiaodan Xing, Yingying Fang, Francisco Herrera, Witold Pedrycz, Simon Walsh, and Guang Yang. Fuzzy attention neural network to tackle discontinuity in airway segmentation. *IEEE Transactions on Neural Networks and Learning Systems*, 2023.
- Minghui Zhang and Yun Gu. Towards connectivity-aware pulmonary airway segmentation. *IEEE Journal of Biomedical and Health Informatics*, 2023.
- Puyang Wang, Dazhou Guo, Dandan Zheng, Minghui Zhang, Haogang Yu, Xin Sun, Jia Ge, Yun Gu, Le Lu, Xianghua Ye, et al. Accurate airway tree segmentation in ct scans via anatomy-aware multi-class segmentation and topology-guided iterative learning. *IEEE transactions on medical imaging*, 2024.
- Kangxian Xie, Jiancheng Yang, Donglai Wei, Ziqiao Weng, and Pascal Fua. Efficient anatomical labeling of pulmonary tree structures via deep point-graph representation-based implicit fields. *Medical Image Analysis*, 99:103367, 2025.
- Wenhao Huang, Haifan Gong, Huan Zhang, Yu Wang, Xiang Wan, Guanbin Li, Haofeng Li, and Hong Shen. Bcnet: Bronchus classification via structure guided representation learning. *IEEE Transactions on Medical Imaging*, 2024.
- Weihao Yu, Hao Zheng, Yun Gu, Fangfang Xie, Jie Yang, Jiayuan Sun, and Guang-Zhong Yang. Tnn: Tree neural network for airway anatomical labeling. *IEEE Transactions on Medical Imaging*, 42(1):103–118, 2022a.
- Syed Ahmed Nadeem, Eric A Hoffman, Alejandro P Comellas, and Punam K Saha. Anatomical labeling of human airway branches using a novel two-step machine learning and hierarchical features. In *Medical Imaging 2020: Image Processing*, volume 11313, pages 234–240. SPIE, 2020b.
- Weiyi Xie, Colin Jacobs, Jean-Paul Charbonnier, and Bram van Ginneken. Structure and position-aware graph neural network for airway labeling. *Medical Image Analysis*, 97:103286, 2024.
- Ngan-Khanh Chau, Truong-Thanh Ma, Woo Jin Kim, Chang Hyun Lee, Gong Yong Jin, Kum Ju Chae, and Sanghun Choi. Branchlabelnet: Anatomical human airway labeling approach using a dividing-and-grouping multi-label classification. *Medical & Biological Engineering & Computing*, pages 1–16, 2024.
- Özgün Çiçek, Ahmed Abdulkadir, Soeren S Lienkamp, Thomas Brox, and Olaf Ronneberger. 3d u-net: learning dense volumetric segmentation from sparse annotation. In *Medical Image Computing and Computer-Assisted Intervention–MICCAI 2016: 19th International Conference, Athens, Greece, October 17-21, 2016, Proceedings, Part II 19*, pages 424–432. Springer, 2016.
- Weihao Yu, Hao Zheng, Minghui Zhang, Hanxiao Zhang, Jiayuan Sun, and Jie Yang. Break: Bronchi reconstruction by geodesic transformation and skeleton embedding. In *2022 IEEE 19th International Symposium on Biomedical Imaging (ISBI)*, pages 1–5. IEEE, 2022b.
- Mie Sato, Ingmar Bitter, Michael A Bender, Arie E Kaufman, and Masayuki Nakajima. Teasar: tree-structure extraction algorithm for accurate and robust skeletons. In *Proceedings the Eighth Pacific Conference on Computer Graphics and Applications*, pages 281–449. IEEE, 2000.
- Kensaku Mori, Shunsuke Ota, Daisuke Deguchi, Takayuki Kitasaka, Yasuhito Suenaga, Shingo Iwano, Yosihori Hasegawa, Hirotsugu Takabatake, Masaki Mori, and Hiroshi Natori. Automated anatomical labeling of bronchial branches extracted from ct datasets based on machine learning and combination optimization and its application to bronchoscope guidance. In *Medical Image Computing and Computer-Assisted Intervention–MICCAI 2009: 12th International Conference, London, UK, September 20-24, 2009, Proceedings, Part II 12*, pages 707–714. Springer, 2009.
- Pechin Lo, Eva M van Rikxoort, Jonathan Goldin, Fereidoun Abtin, Marleen de Bruijne, and Matthew Brown. A bottom-up approach for labeling of human airway trees. *MICCAI Int. WS. Pulm. Im. Anal*, 2011.
- Chenyu Li, Minghui Zhang, Chuyan Zhang, and Yun Gu. Airway labeling meets clinical applications: Reflecting topology consistency and outliers via learnable attentions. *arXiv preprint arXiv:2410.23854*, 2024.
- Frank H Netter. *Atlas of human anatomy, Professional Edition E-Book: including NetterReference. com Access with full downloadable image Bank*. Elsevier health sciences, 2014.
- Michael B Eisen, Paul T Spellman, Patrick O Brown, and David Botstein. Cluster analysis and display of genome-wide expression patterns. *Proceedings of the National Academy of Sciences*, 95(25):14863–14868, 1998.
- Samuel G Armato III, Geoffrey McLennan, Luc Bidaut, Michael F McNitt-Gray, Charles R Meyer, Anthony P Reeves, Binsheng Zhao, Denise R Aberle, Claudia I Henschke, Eric A Hoffman, et al. The lung image database consortium (lidc) and image database resource initiative (idri): a completed reference database of lung nodules on ct scans. *Medical physics*, 38(2):915–931, 2011.

- S. G. Armato III, G. McLennan, L. Bidaut, M. F. McNitt-Gray, C. R. Meyer, A. P. Reeves, B. Zhao, D. R. Aberle, C. I. Henschke, E. A. Hoffman, E. A. Kazerooni, H. MacMahon, E. J. R. Van Beek, D. Yankelevitz, A. M. Biancardi, P. H. Bland, M. S. Brown, R. M. Engelmann, G. E. Laderach, D. Max, R. C. Pais, D. P. Y. Qing, R. Y. Roberts, A. R. Smith, A. Starkey, P. Batra, P. Caligiuri, A. Farooqi, G. W. Gladish, C. M. Jude, R. F. Munden, I. Petkovska, L. E. Quint, L. H. Schwartz, B. Sundaram, L. E. Dodd, C. Fenimore, D. Gur, N. Petrick, J. Freymann, J. Kirby, B. Hughes, A. V. Castele, S. Gupte, M. Sallam, M. D. Heath, M. H. Kuhn, E. Dharaiya, R. Burns, D. S. Fryd, M. Salganicoff, V. Anand, U. Shreter, S. Vastagh, B. Y. Croft, and L. P. Clarke. Data from lidc-idri. The Cancer Imaging Archive, 2015. <https://doi.org/10.7937/K9/TCIA.2015.LO9QL9SX>.
- National Lung Screening Trial Research Team. Reduced lung-cancer mortality with low-dose computed tomographic screening. *New England Journal of Medicine*, 365(5):395–409, 2011.
- National Lung Screening Trial Research Team. Data from the national lung screening trial (nlst). The Cancer Imaging Archive, 2013. <https://doi.org/10.7937/TCIA.HMQ8-J677>.
- Fabian Isensee, Paul F Jaeger, Simon AA Kohl, Jens Petersen, and Klaus H Maier-Hein. nnu-net: a self-configuring method for deep learning-based biomedical image segmentation. *Nature methods*, 18(2):203–211, 2021.
- Thomas N Kipf and Max Welling. Semi-supervised classification with graph convolutional networks. In *International Conference on Learning Representations*, 2017.

## Data Description

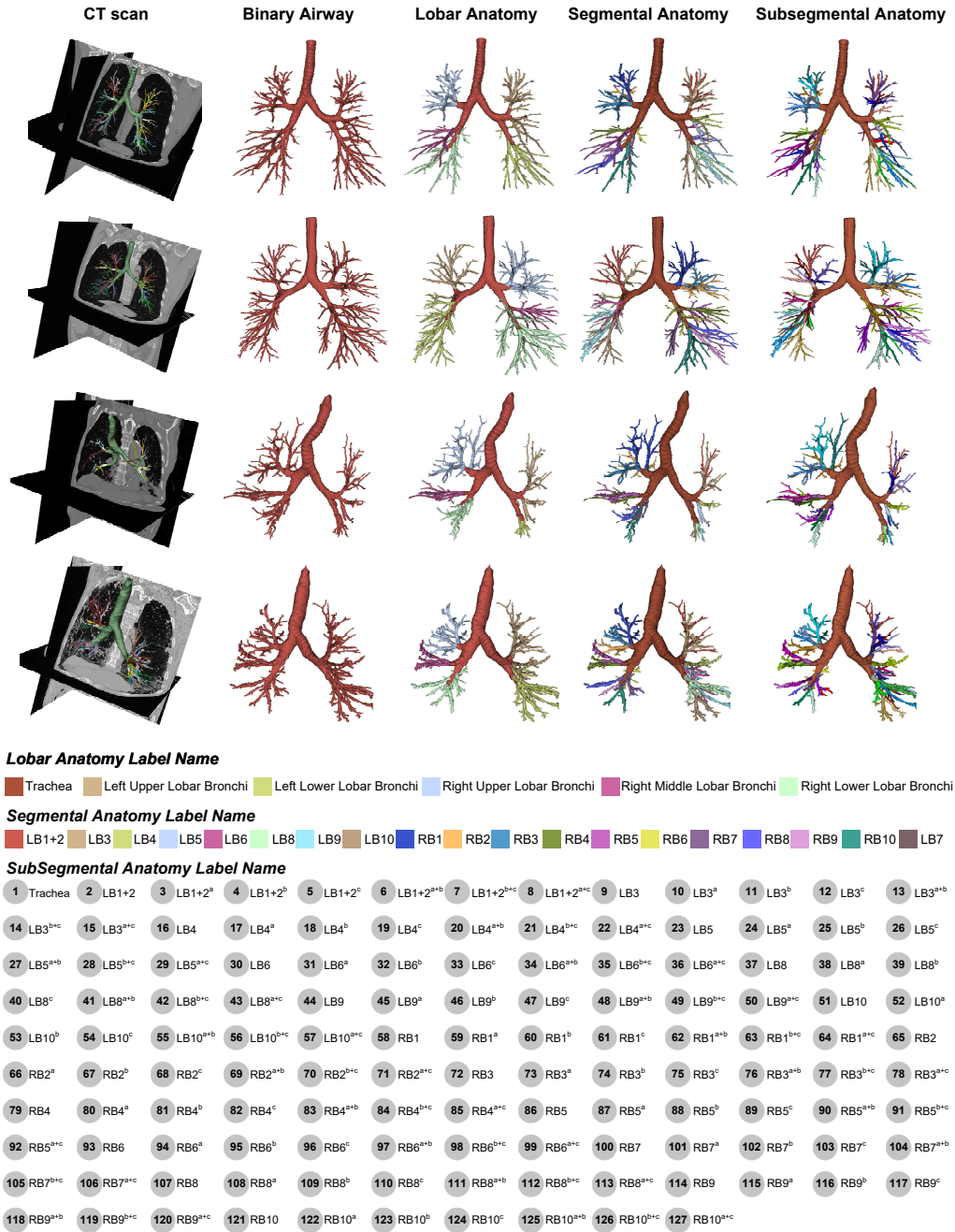


Figure 6: The detailed description of the primary dataset (ATM++). ATM++ consists of paired CT scans and hierarchical airway anatomical structures. The airway anatomies include a binary airway tree, six lobar anatomies, nineteen kinds of segmental anatomies, and one hundred and twenty-seven subsegmental anatomies. Each anatomical structure is clearly labeled with its respective name. Additionally, the first two rows represent the airway anatomies of patients with mild conditions, while the last two rows depict the anatomies of patients with severe fibrosis.